Electronic Supplementary Material (ESI) for Biomaterials Science.

cRGD-targeted gold-based nanoparticles overcome EGFR-TKI resistance of NSCLC via low-temperature photothermal therapy combined with sonodynamic therapy†

Wenhao Lv[a, b], Hao Wu[a, b], Yao Zhang[a], Hui Li[a], Hong Shu[a], Chunhong Su[a], Yangyang Zhu[a, b], Ting Wang[a, b], Fang Nie[a, b*]

[a] *Ultrasound Medical Center, Lanzhou University Second Hospital, Lanzhou, 730000, China;*

[b] *Gansu Province Clinical Research Center for Ultrasonography, Lanzhou, 730000, China;*

Address correspondence to Fang Nie, ery_nief@lzu.edu.cn

Experimental

1. Materials

PLGA-COOH (50:50, molecular weight 7000-17000) and N-hydroxysuccinimide (NHS) were purchased from Yuanye®. Dichloromethane, sodium chloride, gold (III) chloride ($HAuCl_4$), and 1-ethyl-3-(3-dimethylaminopropyl) car-bodiimide hydrochloride (EDAC) were purchased from Sinopharm Chemical Reagent Co., Ltd. Polyvinyl alcohol (PVA) and IR780 were purchased from Sigma-Aldrich®. Sodium citrate dihydrate ($C_6H_5Na_3O_7 \cdot 2H_2O$) and sodium borohydride ($NaBH_4$) were purchased from Aladdin®. Poly(allylamine hydrochloride) was purchased from Macklin®. Hydroxylamine hydrochloride ($NH_2OH \cdot HCl$) was purchased from Beyotime®. Gefitinib was purchased from Selleck®. Cyclic Arg-Gly-Asp-D-Tyr-Glu (RGD) was purchased from Nanjing Peptide Biotech Co., Ltd. All chemicals were used as received without further purification.

2. Cell culture and animals

As confirmed by SPF gene mutation testing, the EGFR-TKI-acquired resistant characteristics of PC-9GR cells were established by increasing the concentration of gefitinib supplemented to the culture medium in a stepwise manner. The cells were cultured in RPMI 1640 medium (Gibco, USA) containing 10% fetal bovine serum (FBS) (Gibco, USA) at 37 °C in a humidified atmosphere with 5% CO_2. To maintain the drug resistance of PC-9GR cells, they were cultured with gefitinib complete medium at a concentration of 8 μM once every 4 generations of passages.

Animals: Male Balb/c nude mice (3-4 weeks) and ICR mice (5-6 weeks) were purchased from Jiangsu Huachuang Xinuo Pharmaceutical Technology Co.

3. Validation of $\alpha_v\beta_3$ overexpression in PC-9GR cells

PC-9 and PC-9GR cells were placed in separate centrifuge tubes (5×10^5 cells) and incubated with

1 μL of $\alpha_v\beta_3$ fluorescent antibody (BN42193R, Biodee) for 20 min, followed by 2 washes with PBS. Blank cells were used as controls, and cells were collected and quantified by flow cytometry (LSR Fortessa, Becton Dickinson, USA). Flow cytometry analysis was performed on FlowJo software (FlowJo, USA).

4. Biosafety assessment of cRGD-GIPG NPs *in vivo*

ICR mice were randomly divided into six groups (n = 3). After injecting different concentrations of cRGD-GIPG NPs (0, 25, 50, 100, 120, 150 μg/mL, 100 μL) into the tail vein, the behavior and survival status of the mice were observed. 14 days later, fresh blood was obtained from each group of mice using eyeball blood sampling, and the blood routine indexes (WBC, RBC, HGB, MCV, MVP, MCHC, HCT, RDW-CV, RDW-SD) were tested. In addition, ICR mice were randomly divided into two groups (n = 3): PBS group (100μL) and the cRGD-GIPG group (2 mg/mL, 100 μL). After 28 days of drug injection via the tail vein, fresh blood was obtained from each group of mice through the same method described above, and each organ function index was tested (ALT, AST, ALB, UREA, CREA, UA).

5. Statistical analysis

Origin and GraphPad software were used for graph production and statistical analysis. Quantitative data are expressed as mean ± standard deviation (SD). Independent samples t-test was used for two-by-two comparison, and one-way ANOVA was used for comparison of multiple sample means, and $P < 0.05$ indicated that the differences were statistically significant.

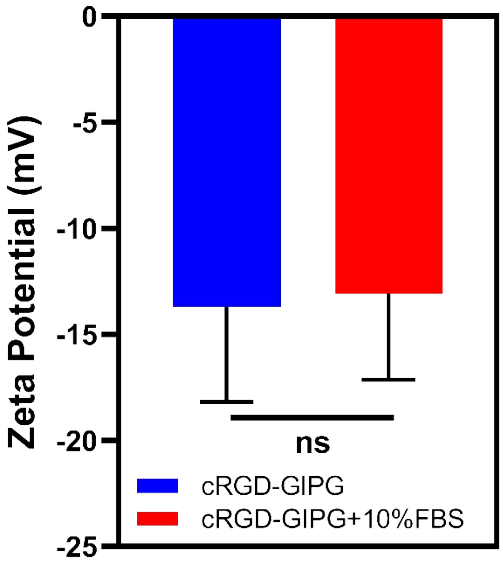

Fig. S1 The potential changes of cRGD-GIPG NPs after interaction with proteins.

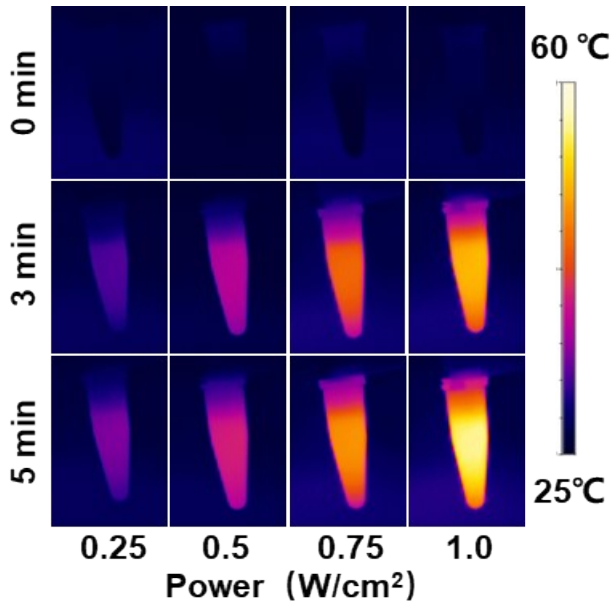

Fig. S2 Infrared thermal photos of cRGD-GIPG NPs (100 μg/mL) irradiated by an 808 nm laser with different power densities.

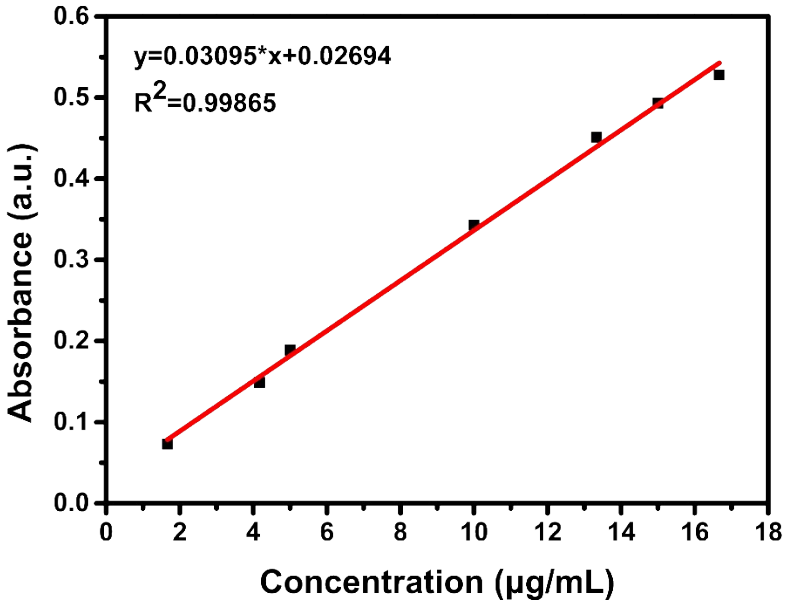

Fig. S3 The standard curve of the UV-vis absorption value of gefitinib at 331 nm versus concentration.

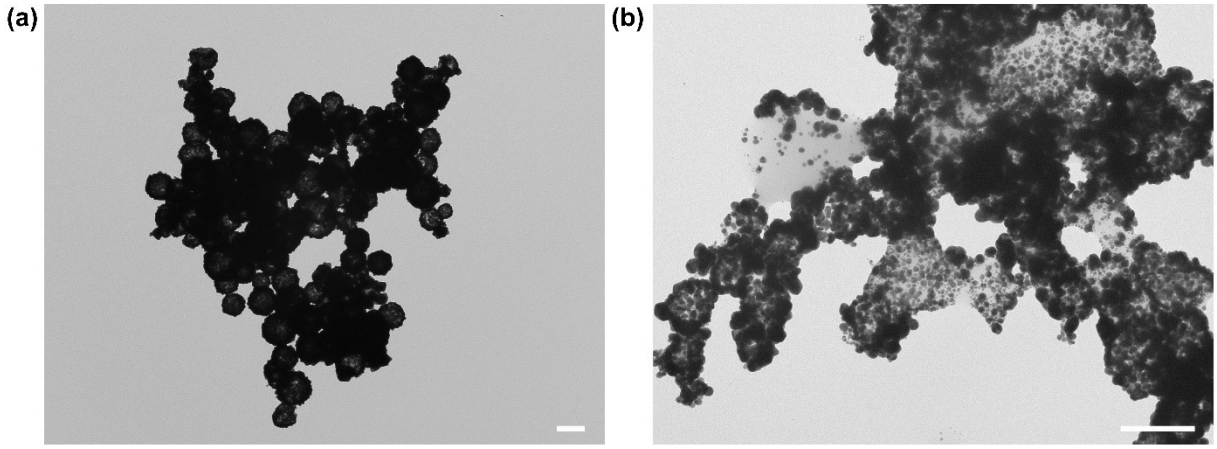

Fig. S4 The TEM images of cRGD-GIPG NPs before (a) and after (b) laser irradiation (808 nm, 0.5 W/cm^2, 5 min) at pH=5.0 (scale bar = 200 nm).

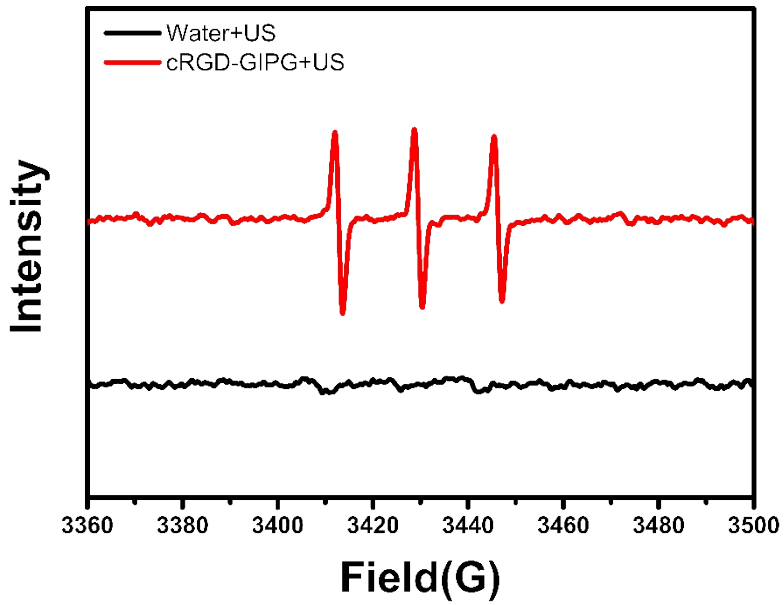

Fig. S5 ESR spectra of water and cRGD-GIPG NPs under US irradiation.

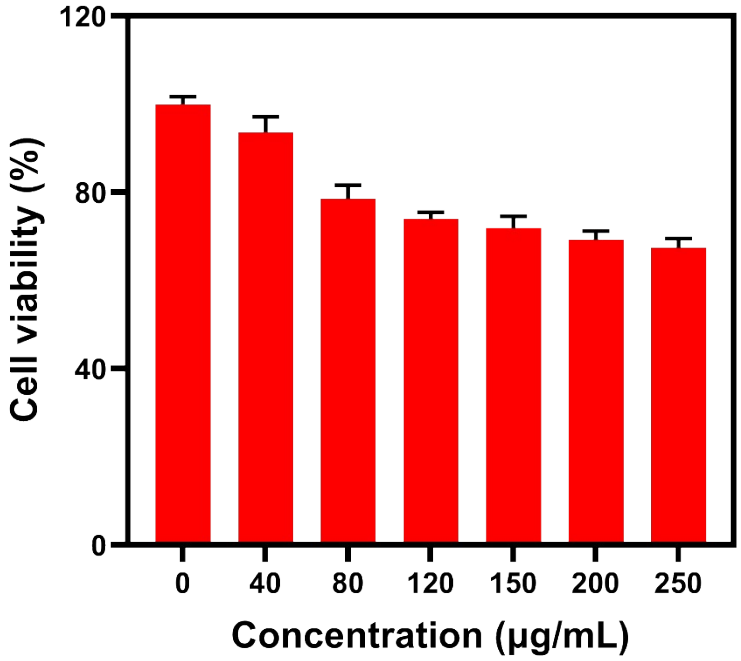

Fig. S6 Cell viability of PC-9GR cells treated with free gefitinib. The concentration of free gefitinib was equal to the amount of gefitinib in cRGD-GIPG NPs. (The horizontal coordinate in the graph is the concentration of cRGD-GIPG NPs.)

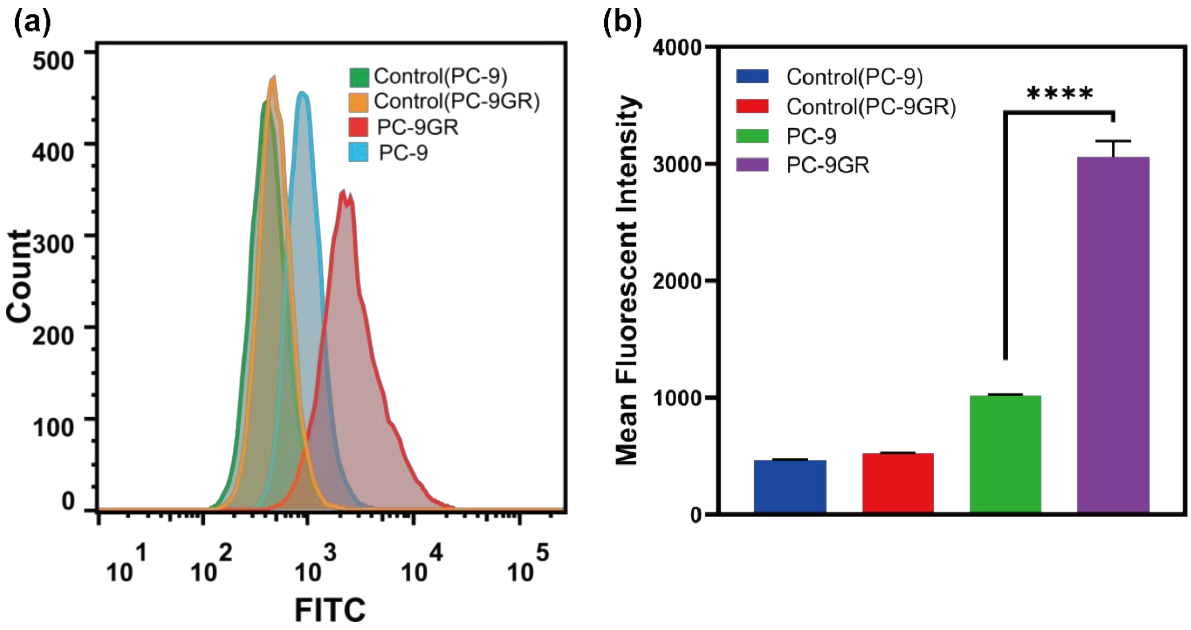

Fig. S7 Flow cytometric analysis (a) and corresponding quantitative results (b) of the $\alpha_v\beta_3$ expression in PC-9 and PC-9GR cells. Data was presented by the mean ± SD, (n = 3). ****$P <$ 0.0001.

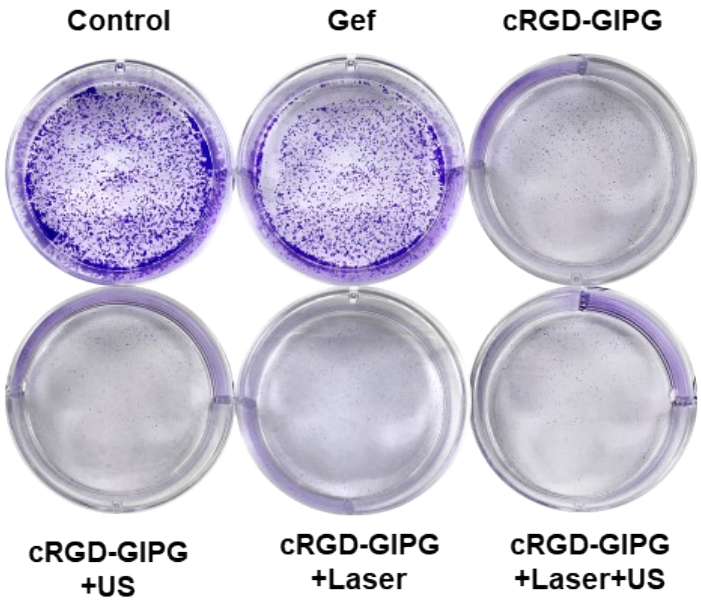

Fig. S8 Colony formation assay of PC-9GR cells with different treatments.

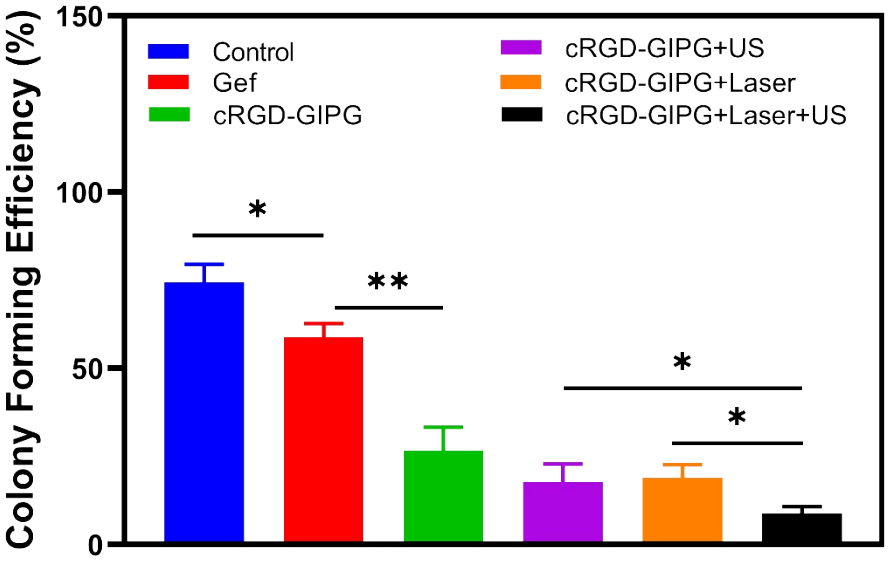

Fig. S9 Colony forming efficiency of PC-9GR cells in various treatment groups. Data was presented by the mean ± SD, $n = 3$. *$P < 0.05$, **$P < 0.01$.

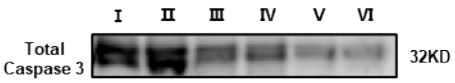

Fig. S10 Western blot analysis of total caspase 3 expressed in PC-9GR cells after different treatments.

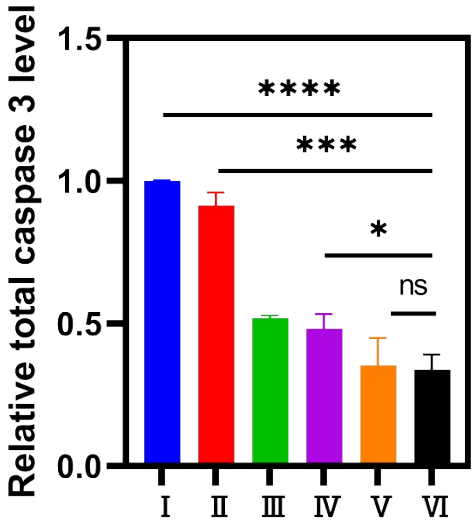

Fig. S11 The corresponding quantification of the total caspase 3 expressed in PC-9GR cells after different treatments. Data was presented by the mean ± SD, $n = 3$. ns, $P \geq 0.05$, *$P < 0.05$, ***$P < 0.001$, ****$P < 0.0001$.

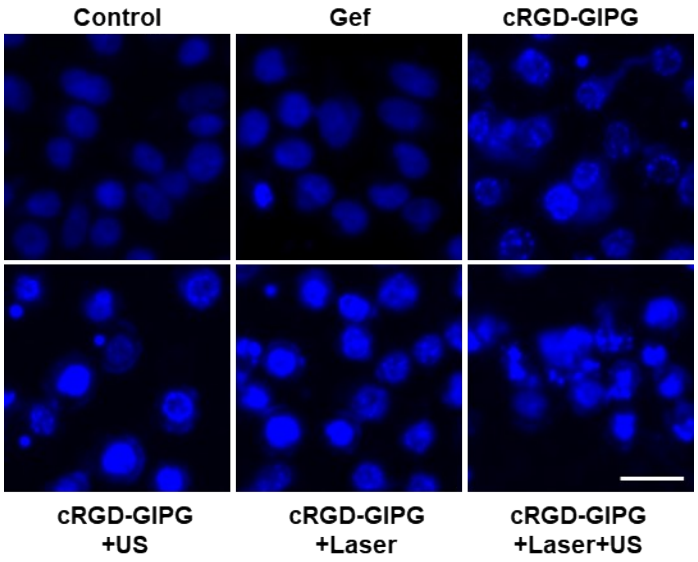

Fig. S12 Fluorescent images of nuclear damage in PC-9GR cells from different treatment groups (scale bar = 50 μm).

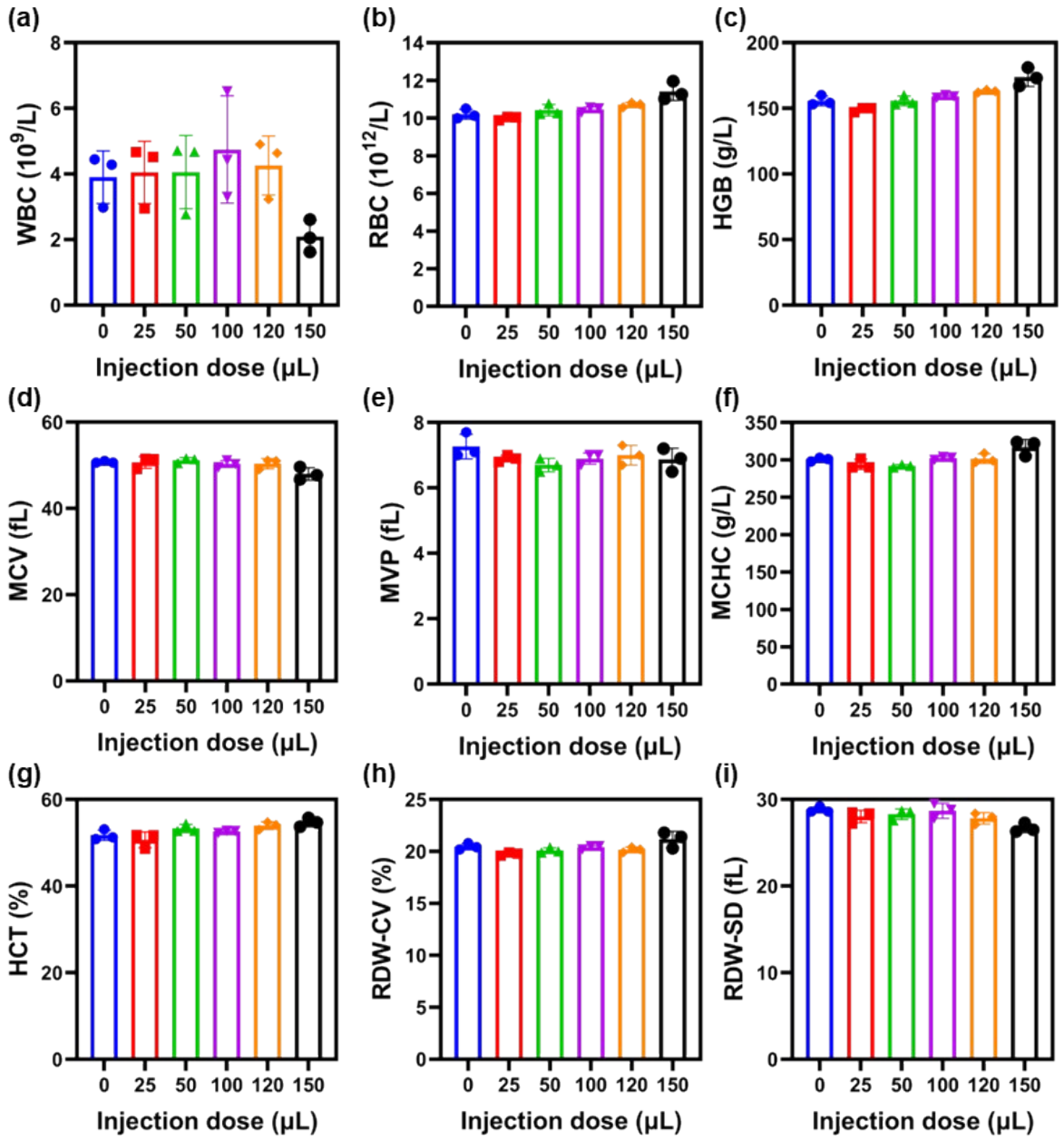

Fig. S13 Various routine blood indices of mice injected with different concentrations of cRGD-GIPG (n = 3).

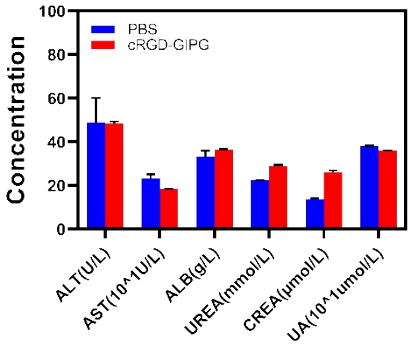

Fig. S14: The functional indices of each organ in different groups (PBS and cRGD-GIPG groups) of mice.

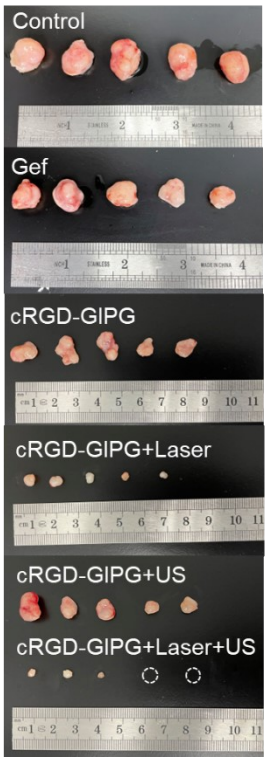

Fig. S15 Photographs of representative tumors dissected from each different treatment group once their treatment has finished.

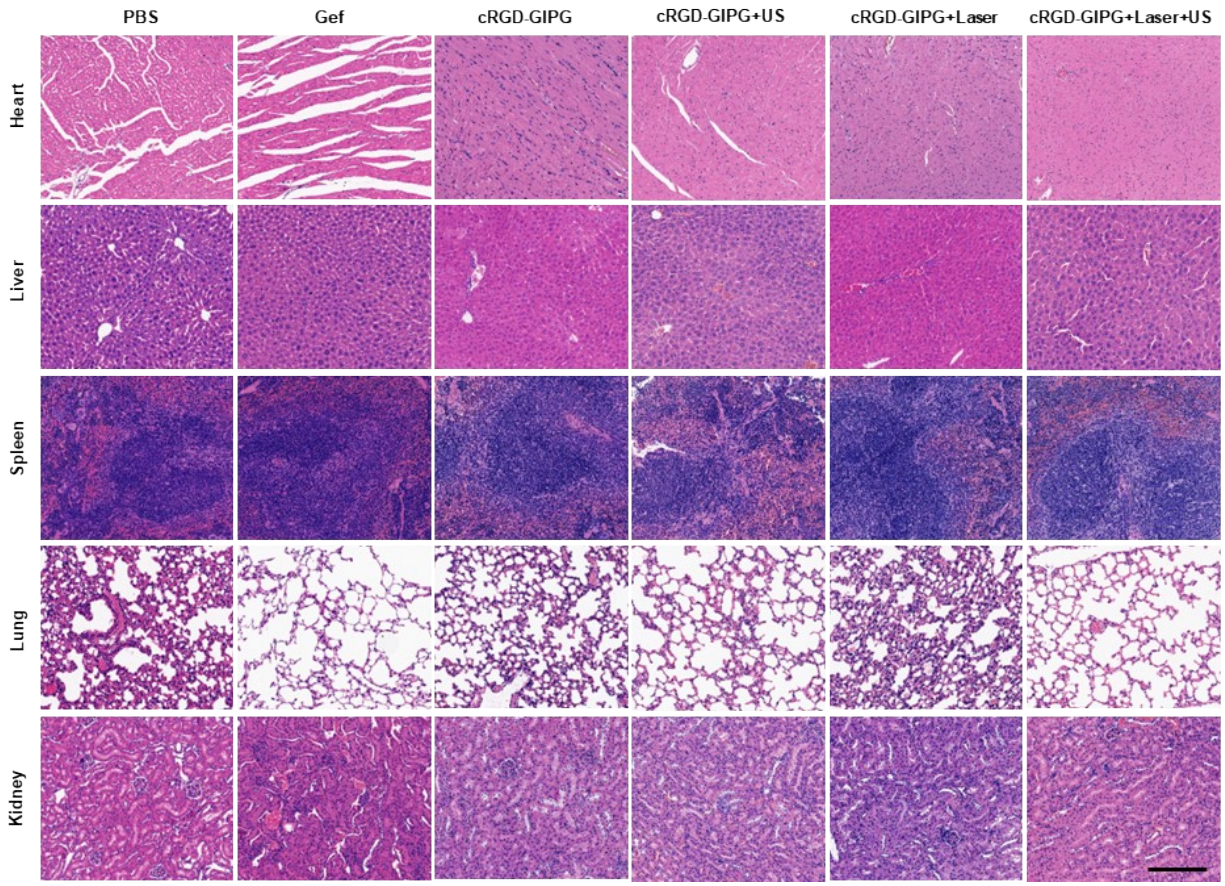

Fig. S16 H & E staining of major organs of different treatments (scale bar = 200 μm).